

Ultrafast chemical-free cell lysis by high speed stream collision induced by surface acoustic waves

Wenbo Wang,^{1,4} Yishan Chen,² Umar Farooq,¹ Weipeng Xuan,¹ Hao Jin, Shurong Dong,^{1,a)} and Jikui Luo^{3,a)}

¹Department of Information Science and Electronics Engineering, Zhejiang University and Cyrus Tang Century for Sensor Materials and Applications, 38 Zheda Road, Hangzhou 310027, China

²Li Dak Sum & Yip Yio Chin Center for Stem Cells and Regenerative Medicine, School of Medicine, Zhejiang University, Zhejiang, Hangzhou 310000, China

³Institute of Renewable Energy and Environmental Technology, University of Bolton, Deane Road, Bolton BL3 5AB, United Kingdom

⁴Southwest China Research Institute of Electronic Equipment, Chengdu 610036, China

(Received 26 January 2017; accepted 23 March 2017; published online 4 April 2017)

This paper reports on a surface acoustic wave (SAW) based cell lysis device on a LiNbO₃ substrate by utilizing high speed collision of cells, which are accelerated by acoustic streaming. With varying working powers, cell lysis was achieved within 20 s and more than 95% lysis efficiency. The cell solution volume effect on SAW based lysis was also investigated and proved that it is not the main issue. With the CCK8 based viability test and verification of cell contents by electrophoresis, the efficient lysis results of our devices have been verified. *Published by AIP Publishing.*

[<http://dx.doi.org/10.1063/1.4979788>]

With the approach of aging society, medical electronic devices and systems have attracted more and more attention in recent years, especially those lab-on-chip, point-of-care, and wearable electronic systems as they can be used to diagnose diseases at an early stage and to monitor real-time health conditions of a person continuously. To satisfy these time-critical demands for point-of-care systems, integrating multiple functional components on a single chip, i.e., a lab-on-a-chip system, would be essential and necessary. Normally, sample preparation is an unnoticeable but indispensable step for lab-on-chip based diagnosis as most tissue samples are living cells with a membrane structure which would block the analysis of the target intracellular molecules such as proteins and nucleic acids. Therefore, cell lysis plays an important role in sample preparation and is meaningful and beneficial for on-chip diagnosis.

There are a few methods to achieve on-chip cell lysis, such as using antibacterial detergent,¹ mechanical cutting,² electrical penetration,³ optical induced lysis,⁴ and acoustic wave lysis.^{5–9} Among them, acoustic wave based lysis devices, especially surface acoustic wave (SAW) based lysis, showed good potential for application due to their merits of high efficiency, short working time, high compatibility, low cost, and easy fabrication. SAW devices are one of the building blocks for modern electronics and have been explored for many applications in communication,¹⁰ sensors,¹¹ and microfluidic devices.^{12,13} For lab-on-a-chip application, SAW devices can be utilized for sensing, streaming, pumping, nebulization, particle manipulation, etc.^{12–17} Since acoustic waves can induce high speed fluidic streaming, it is expected that they could impose or induce strong force on the particles in fluid, which may be utilized to break cell membranes. Indeed, SAW has been utilized for cell lysis

application. Recently, the SAW based lysis study mainly focused on the effect of acoustic pressure on cells. Reboud *et al.* developed a SAW based cell lysis device by streaming induced shear stress.^{5,6} Taller *et al.* integrated a microchannel on the SAW device and obtained continuous cell lysis.⁷ Nevertheless, the investigation of the mechanical impact is still insufficient, and only limited studies have considered to make use of the high speed motion of cells in acoustic streaming. In this study, we report a cell collision based SAW cell lysis device with micro-pillar disruption structures and conduct an investigation to analyze its lysis performance.

Primary mouse embryonic fibroblasts (MEFs) were isolated from E13.5 embryos of C57BL/6J mice. Briefly, head, limbs, visceral tissues, gonads, and vertebral column were removed; the remaining parts were cut into pieces and trypsinized.¹⁸ MEFs were cultured in Dulbecco modified Eagle medium (DMEM) supplemented with 10% fetal bovine serum at 37 °C with 5% CO₂. Passage 1 MEFs with high viability were used in each experiment as cell suspension with a cell density of 2×10^5 cells/ml.

SAW devices were fabricated on 128° Y-cut LiNbO₃ substrates with Cr/Au (5 nm/60 nm thickness) interdigitated electrodes (IDT) formed by lithography and lift-off process. The acoustic aperture was set to 4 mm in order to obtain a wide acoustic lysis region. The wavelengths of the devices were set to 80 and 100 μm with 30 pairs of 20 and 25 μm width fingers, respectively.

For cell lysis, a SU8 2150 (Microchem, USA) photoresist was utilized to build the fluid chamber with the size of 7×7 mm² (acoustic wave propagation area in front of the IDTs) and micro-pillar structures as shown in Fig. 1(c). The thickness (height) of SU8 structures is approximately 110 μm with a good perpendicularity. The width of the chamber walls is 100 μm. Micropillars with sharp edges were fabricated for the mechanical impact with cells, which have a fixed size of 50 μm × 50 μm. The number of

^{a)}Authors to whom correspondence should be addressed. Electronic addresses: dongshurong@zju.edu.cn and jk2@bolton.ac.uk

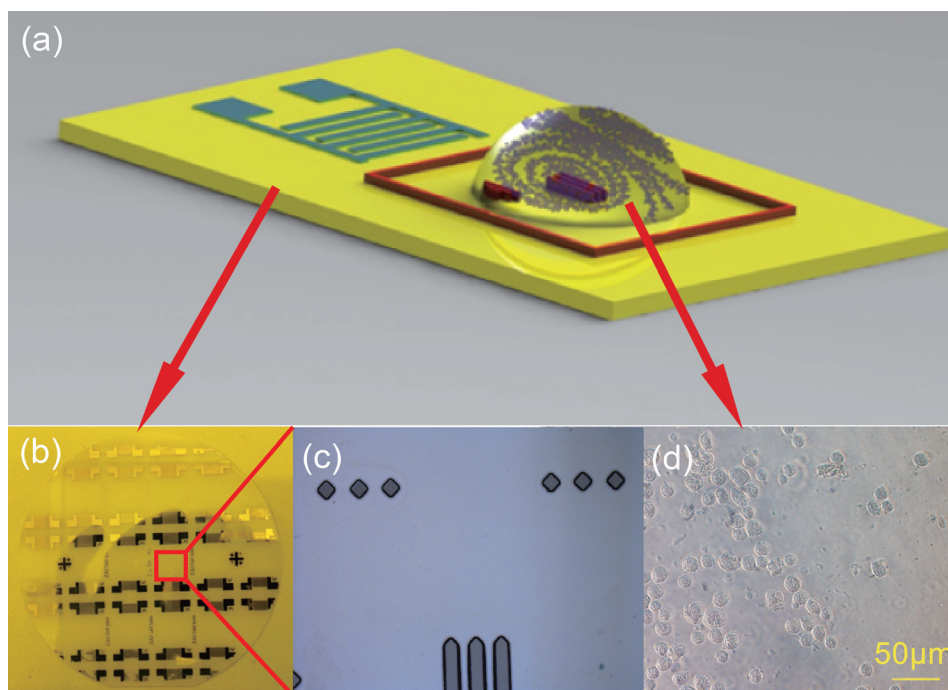


FIG. 1. Schematic drawing of the SAW based cell lysis device working mechanism (a); lysis device wafer (b); the microscopy view of SU8 collision structures (c); microscopy image of target cells: C57BL/6J E13.5 mouse embryonic fibroblast (d).

pillars is 5–8 with a separation of 100 μm between them. No specific treatment was conducted for the surface of the chamber and the piezoelectric substrate to reduce possible adsorption of cells or intercellular contents as the lysates were taken out immediately for other analysis once lysis completed.

A network analyzer (E5071C, Agilent, USA) was used to characterize the transmission and reflection properties of the fabricated SAW devices. During the lysis process, a signal generator (SP2461, China) was used to apply the RF signal at the resonant frequency of the SAW devices, the RF signal was amplified by an RF power amplifier (MW1980-50 W, China), and the output power amplitude was also measured and ascertained by a power meter integrated in the RF amplifier.

To obtain cell lysis, cell solution droplets were added to the SU8 chamber with a pipette of varying volumes. Then, the RF power signal in the range of 1 to 6.3 W was applied to the devices. Very high speed acoustic streaming was induced, and the cells were actuated to move with the stream and impact to the SU8 micro-pillars, which would easily destroy the cell membranes, leading to cell lysis. The lysis time was set to 20 s, and after the lysis, the lysates were taken out with a pipette to analyze. The SAW devices were put on an Aluminum heat sink to remove heat and to maintain the chamber temperature lower than 40 °C (confirmed by an infrared camera) at which no measurable heat-induced cell lysis was observed.

To distinguish the live cells from the dead ones, Trypan blue dyeing was applied to the lysates. Trypan blue could not penetrate through the cell membrane so that only dead cells would be dyed due to the broken membrane of the cells. After dyeing, in the microscopy view as shown in Fig. 3, live cells maintained their initial white color, and the dead cells were dyed blue. After dyeing, both lysate and cell solutions were loaded into a haemocytometer (Neubauer improved) for cell counting and lysis efficiency calculation.

For the verification of cell lysis, a Cell Counting Kit-8 (CCK8, SAB Company, USA) was used to assess the lysis effect on the viability of MEFs. After cell lysis, cell lysate of each group was taken in a 96-well plate and the CCK-8 reagent was added with 1:10 (v/v) per 100 μl medium. The suspension of living cells was measured as the control group for further characterisation. All the cells were further cultured in the incubator for 4 h before the endpoint of incubation. The optical density (OD) at 450 nm was determined for the supernatant of each well using a microplate reader (SpectraMax 190, Molecular Devices, USA). With each time in triplicate, experiments were performed at least three times.

Electrophoresis was also utilized to check the release of nucleic acid from the cracked cells. Briefly, SAW-treated and untreated cell suspensions were centrifuged at 300 g for 5 min. 10 μl of supernatants without cells/cell debris were collected as samples for gel electrophoresis.

The transmission and reflection properties of SAW devices used for lysis are illustrated in Fig. 2; both 80 and 100 μm devices show a good Rayleigh resonant peak at ~49.0 and ~38.7 MHz, respectively. The insertion loss of both the devices is similar with a value of ~-10 dB, not the best performance, but would be sufficient for this lysis experiment. When a droplet was placed in the chamber, acoustic energy was coupled into the liquid, and no resonant peak in the S21 spectrum was observed as shown in Ref. 16.

The electromechanical coupling coefficient (K^2) can be used to estimate the piezoelectric performance of SAW devices. SAW devices with larger K^2 would be superior to convert electrical energy into mechanical vibration, which is especially important for actuation applications like microfluidics.¹⁹ For cell lysis applications, it can be expected that devices with larger K^2 values would induce higher acoustic streaming velocity, leading to better and more efficient cell destruction. The K^2 values can be calculated using the following equation:²⁰

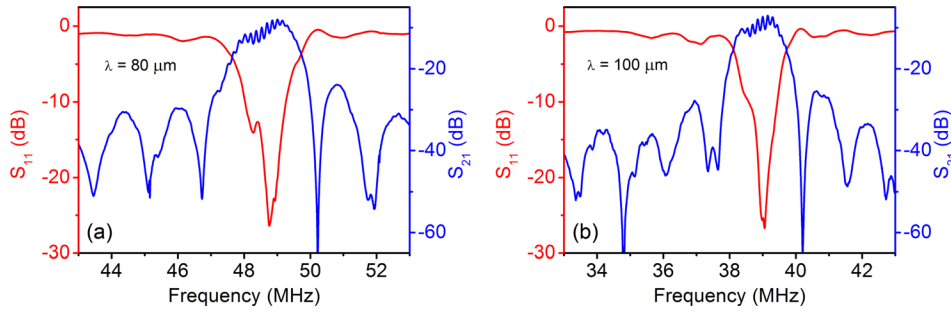


FIG. 2. Transmission (S_{21}) and reflection (S_{11}) spectra of 80 and 100 μm wavelength devices (a) and (b).

$$K^2 = \frac{\pi G_m(f_r)}{4NB_s(f_r)}, \quad (1)$$

where N is the number of finger pairs, $G_m(f_r)$ and $B_s(f_r)$ are the motional conductance and static susceptance at the resonant frequency, f_r , respectively; both the values can be obtained from the Smith chart of RF measurements. The K^2 values are $\sim 1.83\%$ and $\sim 1.86\%$ for the devices with the wavelength of 80 and 100 μm , respectively, which are smaller than those of the reported LiNbO_3 SAW devices (2–4%)²¹ but larger than the most reported well-worked piezoelectric thin film based SAW microfluidic devices,^{16,17} indicating that our devices can be well expected in microfluidic performance. It is also noted that devices with different wavelengths have quite similar K^2 values as the wavelength difference in these devices is small compared to the thickness of the LiNbO_3 substrate. The streaming velocity of the devices was not investigated in this work. From the previous works, it is estimated that the streaming velocity is about 10–20 cm/s at an RF power of 4 W and it may decrease slightly due to the existence of micro-pillars. As the pillar

height (110 μm) is much smaller than the droplet height (1.0–2.0 mm) and the liquid flows up-forward at the Rayleigh angle, the forward streaming velocity does not change much, while the reverse streaming velocity would be affected slightly²² (impact with micropillars). The surface displacement induced by SAW is directly responsible for the streaming, which can be estimated by $\frac{A}{\lambda} = 8.15 \times 10^{-6} P^{0.225} + 5 \times 10^{-6} P^{0.8}$,²³ where P is the RF power in Watts. At powers of 1, 4, and 6.3 W, the displacements are 1.1, 2.1, and 2.7 nm for 80 μm devices and 1.3, 2.6, and 3.4 nm for 100 μm devices, respectively.

Cell solutions were lysed by both 80 and 100 μm wavelength SAW devices with increasing RF power from 0 to 6.3 W. The lysates were then taken out with a pipette and dyed with Trypan blue. The microscopy images of lysates are shown in Fig. 3 in order to get a better understanding of the lysis results and its efficiency, while their exact data are given in Fig. 4(a). It is obvious that a threshold power exists for the lysis process. When the RF power is less than 1 W, both the devices show poor lysis efficiency ($<15\%$) and most cells are white in the microscopic view, i.e., they are

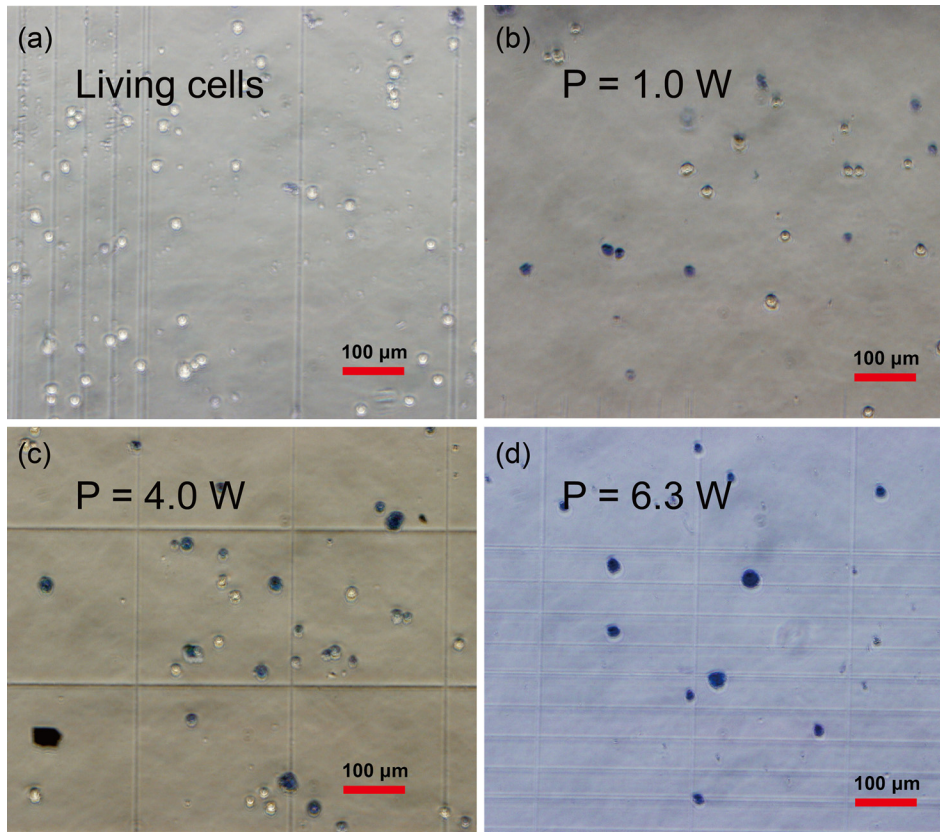


FIG. 3. Microscopy image of cell lysates with varying RF power from 0 to 6.3 W (a)–(d) with Trypan blue dyeing; alive cells maintain their initial white color, and the broken cells were dyed blue.

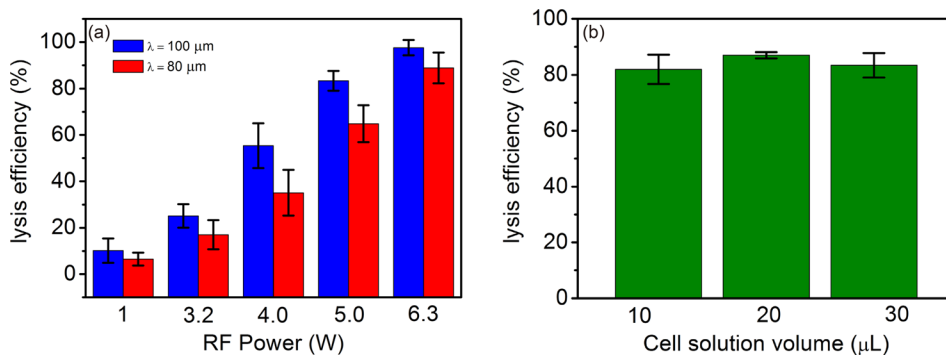


FIG. 4. Cell lysis efficiency as a function of RF power (a) and droplet volume (b).

alive. Lysis efficiency increases with increasing RF power as a positive nonlinear correlation. When the RF power reaches 6.3 W, the microscopy view shows entire blue-colored cells, i.e., almost all the cells are lysed. A lysis efficiency of 95% is obtained. It is also noted that for all the working powers, 100 μm devices perform better than those with 80 μm wavelength, which is due to the fact that longer wavelength can induce higher surface vibration in the acoustic propagation path and have stronger streaming effect for the droplet.^{22,24} It should be pointed out that cell lyses occur when there is no micropillar in the chamber, mostly induced by the impact of cells on the SU8 walls, but the efficiency is less than 20%, much smaller than those induced by the micropillars as such we focused on the lysis using micropillars. Compared with other phononic lattice or channel based SAW lysis,^{5–7} our devices demonstrate a comparable lysis efficiency (38%–98% for other researchers) but with a larger working power (0.8–2 W for other researchers). The requirement for higher powers for our cell lysis is mainly due to the relatively poor performance of the SAW device and lower K^2 values as shown in Fig. 2. Lower RF powers are expected to achieve higher cell lysis efficiency if high performance SAW devices are used, and this is under development. Although the efficiency value is slightly less than conventional detergent lysis,²⁴ it is comparable or superior to other on-chip lysis methods like electrical lysis or optical induced lysis.^{3,4} The volume effect on cell lysis efficiency was investigated. Since the surface of LiNbO₃ is hydrophilic, liquid spreads over the chamber easily under SAW excitation. The high volume liquid resulted in a higher liquid level, and the chamber wall is mostly for preventing the liquid spread out. Although the streaming velocity varies slightly when the liquid volume changes, the results showed that within the volume region of several tens of μL s, there is no significant difference in the lysis efficiency as shown in Fig. 4(b).

The ratio of R_d/l_{SAW} is also a non-negligible issue for streaming efficiency,²² where R_d is the radius of the droplet, and l_{SAW} is the attenuation length of the Rayleigh wave, which can be estimated as^{25,26}

$$\alpha_l = \frac{1}{l_{\text{SAW}}} = \frac{\rho_f c_f}{\rho c \lambda}, \quad (2)$$

where ρ_f and ρ are the densities of the fluid and the substrate, c_f is the longitude wave velocity in the fluid, and c is the velocity in the substrate.²² At $\alpha_l > 1$, the acoustic energy attenuates quickly and completely absorbed by liquid; at $\alpha_l < 1$, the acoustic energy would not be coupled into the fluid, reducing streaming efficiency. For both 80 and 100 μm wavelengths, the ratio is around 2 and the acoustic energy could be coupled into liquid efficiently for both the devices.

Fig. 5(a) shows the relative cell viability of lysates with different RF powers. With the increase in power, cell viability dramatically drops and approaches zero at 6.3 W, clearly indicating that the target cells are indeed lysed by acoustic streaming. This was also verified by the electrophoresis results as shown in Fig. 5(b). The nucleic acid in the cracked cells is released in the supernatant, which shows a wide band in agarose, while the supernatant medium of alive cells presents none of this. Lysates could be further used as templates for PCR amplification, which is vitally beneficial for most DNA based bio-analyses in lab-on-a-chip applications for point-of-care diagnosis. Considering the above results, it is sure that our devices achieved sufficient cell lysis. The lysis time was fixed at 20 s for the work reported here, and it was found that when the power is below the threshold value, no matter how long the time is, cell lysis would not occur or complete. When the power is above the threshold value, the time would be positively related to the lysis efficiency. It is also worth mentioning that the droplet dimension and the

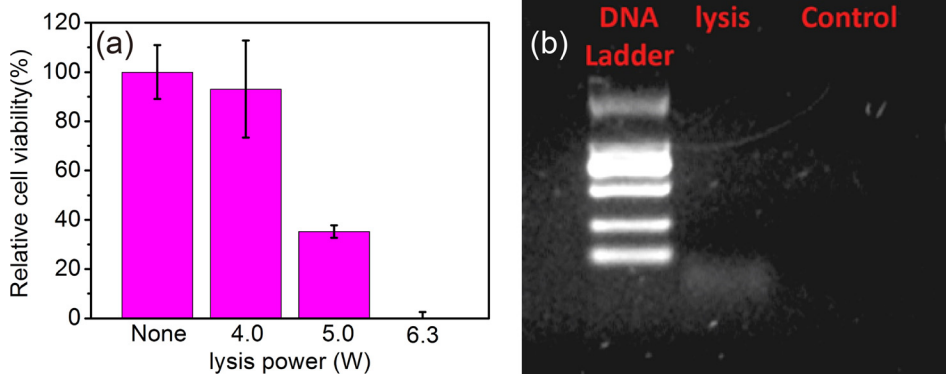


FIG. 5. Relative cell viability for lysates with different RF powers (a) and electrophoresis images of the supernatant from lysates and living cell suspension (control group) (b). DNA Ladder: 100, 250, 500, 750, 1000, 200 bp (DL2000, Takara).

position would affect the streaming pattern and efficiency and hence the lysis efficiency, and these will be reported in the future.

In conclusion, this study explored a SAW based cell lysis device for chemical-free bio-sample preparation. The proposed device was based on acoustic streaming induced collision. Within a working time of 20 s, more than 95% lysis efficiency was achieved, and the results were verified by the CCK8 based viability test and electrophoresis. This device provides an alternative method for on-chip cell lysis which is an important component for microfluidic systems, considering the good compatibility with the conventional electronic system; SAW based cell lysis can be expected to have promising potential in future point-of-care lab chip systems.

This project was supported by NSFC (Nos. 61274037, 61301046, and 61376118) and “the Fundamental Research Funds for the Central Universities 2016XZZX001-05.” The authors also acknowledge the Innovation Platform of Micro/Nanodevices and Integration System, Zhejiang University.

- ¹M. A. S. Aly, M. Gauthier, and J. Yeow, *Biomed. Microdevices* **18**, 2 (2016).
- ²S.-S. Yun, S. Y. Yoon, M.-K. Song, S.-H. Im, S. Kim, J.-H. Lee, and S. Yang, *Lab Chip* **10**, 1442 (2010).
- ³N. de Lange, T. M. Tran, and A. R. Abate, *Biomicrofluidics* **10**, 024114 (2016).
- ⁴S. H. Huang, L. Y. Hung, and G. B. Lee, *Lab Chip* **16**, 1447 (2016).
- ⁵J. Reboud, Y. Bourquin, R. Wilson, G. S. Pall, M. Jiwaji, A. R. Pitt, A. Graham, A. P. Waters, and J. M. Cooper, *Proc. Natl. Acad. Sci. U. S. A.* **109**, 15162 (2012).
- ⁶A. Salehi-Reyhani, F. Gesellchen, D. Mampallil, R. Wilson, J. Reboud, O. Ces, K. R. Willison, J. M. Cooper, and D. R. Klug, *Anal. Chem.* **87**, 2161 (2015).

- ⁷D. Taller, K. Richards, Z. Slouka, S. Senapati, R. Hill, D. B. Go, and H. C. Chang, *Lab Chip* **15**, 1656 (2015).
- ⁸L. T. Wang, Y. J. Li, A. Lin, Y. Choe, M. E. Gross, and E. S. Kim, *J. Microelectromech. Syst.* **22**, 542 (2013).
- ⁹T. J. Lyford, P. J. Millard, and M. P. D. Cunha, *Ultrasonics Symposium (IUS), IEEE International* **2012**, 1216–1219 (2012).
- ¹⁰J. Koike, K. Shimoe, and H. Ieki, *Jpn. J. Appl. Phys., Part 1* **32**, 2337 (1993).
- ¹¹W. Xuan, M. He, N. Meng, X. He, W. Wang, J. Chen, T. Shi, T. Hasan, Z. Xu, Y. Xu, and J. K. Luo, *Sci. Rep.* **4**, 7206 (2014).
- ¹²L. Y. Yeo and J. R. Friend, *Biomicrofluidics* **3**, 12002 (2009).
- ¹³L. Y. Yeo and J. R. Friend, *Annu. Rev. Fluid Mech.* **46**, 379 (2014).
- ¹⁴D. S. Brodie, Y. Q. Fu, Y. Li, M. Alghane, R. L. Reuben, and A. J. Walton, *Appl. Phys. Lett.* **99**, 153704 (2011).
- ¹⁵Y. Q. Fu, J. K. Luo, X. Y. Du, A. J. Flewitt, Y. Li, G. H. Markx, A. J. Walton, and W. I. Milne, *Sens. Actuators, B* **143**, 606 (2010).
- ¹⁶W. Wang, X. He, J. Zhou, H. Gu, W. Xuan, J. Chen, X. Wang, and J. K. Luo, *J. Electrochem. Soc.* **161**, B230 (2014).
- ¹⁷J. Zhou, M. DeMiguel-Ramos, L. Garcia-Gancedo, E. Iborra, J. Olivares, H. Jin, J. K. Luo, A. S. Elhady, S. R. Dong, D. M. Wang, and Y. Q. Fu, *Sens. Actuators, B* **202**, 984 (2014).
- ¹⁸E. Lujan, S. Chanda, H. Ahlenius, T. C. Südhof, and M. Wernig, *Proc. Natl. Acad. Sci. U. S. A.* **109**, 2527 (2012).
- ¹⁹W. B. Wang, Y. Q. Fu, J. J. Chen, W. P. Xuan, J. K. Chen, X. Z. Wang, P. Mayrhofer, P. F. Duan, A. Bittner, U. Schmid, and J. K. Luo, *J. Micromech. Microeng.* **26**, 075006 (2016).
- ²⁰W. R. Smith, H. M. Gerard, J. H. Collins, T. M. Reeder, and H. J. Shaw, *IEEE Trans. Microwave Theory Tech.* **17**, 856 (1969).
- ²¹C. Chien-Chuan, H. Rong-Chang, and C. Ying-Chung, *IEEE Trans. Ultrason. Ferroelectr. Freq. Control Soc.* **48**, 387 (2001).
- ²²M. Alghane, Y. Q. Fu, B. X. Chen, Y. Li, M. P. Y. Desmulliez, and A. J. Walton, *J. Appl. Phys.* **112**, 084902 (2012).
- ²³K. Chono, N. Shimizu, Y. Matsui, J. Kondoh, and S. Shiokawa, *Jpn. J. Appl. Phys., Part 1* **43**, 2987 (2004).
- ²⁴J. Berlowska, M. Dudkiewicz, D. Kregiel, A. Czyzowska, and I. Witonska, *Enzyme Microb. Technol.* **44**, 75–76 (2015).
- ²⁵L. Schmid, A. Wixforth, D. A. Weitz, and T. Franke, *Microfluid. Nanofluid.* **12**, 229 (2012).
- ²⁶R. M. Arzt, E. Salzmann, and K. Dransfeld, *Appl. Phys. Lett.* **10**, 165 (1967).